Korean Journal of Remote Sensing, Vol.23, No.3, 2007, pp.199~209

Building Extraction from Lidar Data and Aerial Imagery using Domain Knowledge about Building Structures

Suyoung Seo †

GeoResources Institute, Mississippi State University, MS State, MS 39762

Abstract : Traditionally, aerial images have been used as main sources for compiling topographic maps. In recent years, lidar data has been exploited as another type of mapping data. Regarding their performances, aerial imagery has the ability to delineate object boundaries but omits much of these boundaries during feature extraction. Lidar provides direct information about heights of object surfaces but have limitations with respect to boundary localization. Considering the characteristics of the sensors, this paper proposes an approach to extracting buildings from lidar and aerial imagery, which is based on the complementary characteristics of optical and range sensors. For detecting building regions, relationships among elevation contours are represented into directional graphs and searched for the contours corresponding to external boundaries of buildings. For generating building models, a wing model is proposed to assemble roof surface patches into a complete building model. Then, building models are projected and checked with features in aerial images. Experimental results show that the proposed approach provides an efficient and accurate way to extract building models.

Key Words : Co-registration, Building Extraction, Contour Graph, Surface Adjacency, Wing Model, Data Fusion.

1. Introduction

Because of importance of building models in spatial information systems, rigorous studies have been performed on building extraction in the fields of photogrammetry and computer vision (Brunn *et al.*, 1998; Fischer *et al.*, 1998; Mckeown *et al.*, 1999; Ameri, 2000). Previous studies have shown that there are difficulties in building extraction because of the incompleteness of features extracted from sensory input data and the complexity of building structures. From the previous studies, however, it has been proven efficient to integrate multiple sensory input data using complementary characteristics among different sensors, reducing problems caused by missing features and by complexity of building structures. (Abidi and Gonzalez, 1992).

Hence, in this paper, a building extraction approach which exploits the complementary characteristics of optical and range sensors is proposed. Also, domain knowledge about building models is integrated together to generate suitable

Received 9 June 2007; Accepted 13 June 2007.

† Corresponding Author: Suyoung Seo (suyoung@erc.msstate.edu)

building models.

2. Backgrounds

During last decades, building extraction has been studied extensively with various types of data. Considering previous studies, it is obvious that their approaches are closely related with data types employed for building extraction. Accordingly, it would be desirable to understand previous studies with data types and methodologies being classified. Data types used for building extraction can be divided into two broad sensors: optical and range data. The most promising approaches, however, are based on the combination of multiple sensory data. Thus, approaches based on data fusion are reviewed in the following for further investigation.

1) Building Detection by Data Fusion

For detecting building regions, various sensory data have been combined together such as elevations, multispectral and intensity images. Csatho *et al.* (1999) described a general strategy to detect buildings using multi-sensor data sets, whereby aerial images, lidar data and multi-spectral images are exploited. Mckeown *et al.* (1999) presented a method using features derived from the stereo-based and classification-based extraction. They detected building regions from hyperspectral imagery and DSMs (Digital Surface Models) such that the process prunes line segments which are not likely to be building boundaries, reducing the number of false positives significantly. Tao and Yasuoka (2002) utilized heuristic knowledge about the quality of object surfaces with respect to sensors. Pixel values derived from color infra-red IKONOS images and DSM data were used together for knowledge-based classification. Haala and Brenner (1999) merged a DSM and multispectral data at the pixel level and then applied ISODATA classification. After classification, most objects including buildings, trees, and grass-covered areas were detected well.

2) Building Reconstruction by Data Fusion

In data fusion-based approaches to building reconstruction, various types of data such as aerial images, lidar data, ground plans, and multispectral images have been combined.

Ground plans from topographic maps or GIS data were used to initiate the external boundaries of buildings (Brenner and Haala, 1998; Vosselman and Dijkman, 2001), where surface patches were initiated based on ground plans and refined with lidar data. Ground plans were decomposed into rectangular regions and then laser points within the rectangles were clustered based on the segmented patches. Plane parameters of the patches were estimated using a Hough transform method and least- squares method. From the experiments, complex roof structures were shown to be reconstructed successfully by refining surface patches with a split-and-merge process of lidar points and finally by outlining the surfaces with ground plans.

Mckeown *et al.* (1999) utilized hyperspectral and panchromatic images for building extraction. They generated a class map from HYDICE images and utilized that to discard invalid hypotheses modeled from panchromatic imagery. In addition, material types of the roof surfaces were identified based on the texture information derived from the class map. Ameri (2000) combined DSM data and aerial images for building reconstruction, whereby planar surface patches were extracted from a DSM and combined for modeling buildings. Then building model hypotheses were checked with edge pixels in aerial images.

Table 1. Framework of the building extraction approach proposed.

Process	Lidar Data	Aerial Images	Output
Co-registration	3D lines	3D image points	EOPs of aerial images
Building Detection	Contours and adjacency graphs		Building roof boundaries
Building Model Generation	3D surface patches and adjacency graphs		Hypothesized building models
Building Model Verification		2D edge lines	Verified/refined building models

3) Framework of This Study

In this study, a data fusion-based method is proposed to extract building models using lidar and aerial images. As compared with previous studies using multiple sensory data (Ameri, 2000), the method proposed exploits domain knowledge about building structures in building detection and modeling. The building extraction approach is composed of four main processes: 1. Co-registration, 2. Building detection, 3. Building model generation, and 4. Building model verification. Table 1 summarizes the properties of each task in terms of sensors, features and outputs.

Firstly, in co-registration, aerial images are oriented using control features present in lidar data. Secondly, in building detection, contours are analyzed to detect the occurrence of buildings. The detection is based on contour graphs. Thirdly, in building model generation, 3D surface patches from lidar data are used, whereby building models are generated based on topological and geometric relationships among surface patches. Finally, in building model verification, topology and geometry of the building models are verified with features existing in aerial images.

3. Co-registration

A crucial part in applications using multiple sensory input data is to establish a common reference frame, also known as sensor alignment or sensor registration. The registration process in this study is based on sensor invariant features, whereby features

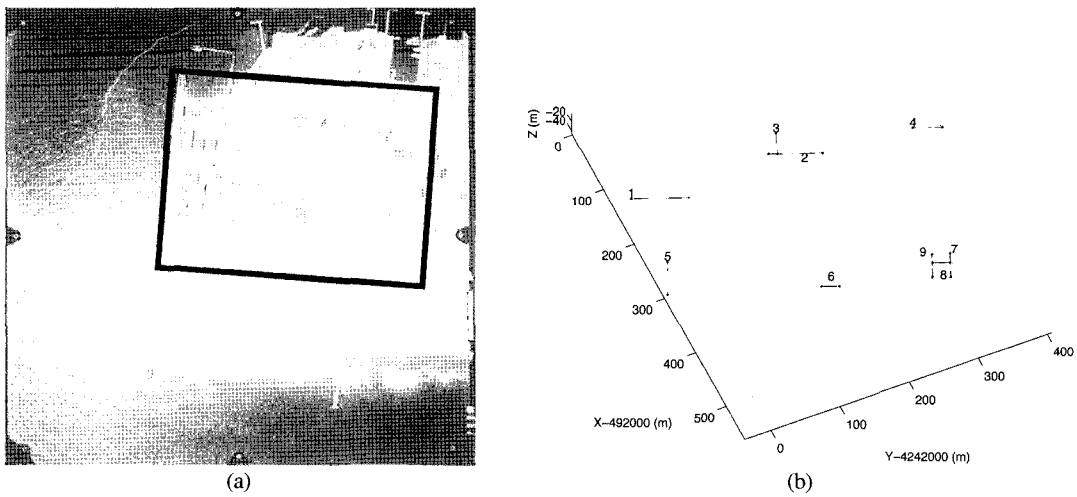

(a) (b)

Fig. 1. Aerial image and line features from lidar data. In (a), the box shows the data extent of lidar data where control features were collected. (b) displays the control line features extracted from the ridge lines of building roofs.

commonly existing in the different data sets are exploited (Schenk and Csatho, 2002).

In this study, aerial images which are not oriented and lidar data which are registered to object space over an urban area in Ocean City, Maryland were used. Detail information about the data set is described in Csatho *et al.* (1998). Given aerial photographs were scanned at 24 μm. Data area covered by lidar area is shown by the rectangular box in Fig. 1-a, where the point density of lidar data is 1.2 points/m^2.

To perform co-registration of the given two sensory data, the aerial images were chosen to be oriented using control features available in lidar data. From visual inspection of the data sets, building ridge lines shown in Fig. 1-b were exploited as control features because of their high accuracy across the study area. Exterior orientation parameters of a pair of aerial images were figured out based on collinear equations, whereby the position and attitude parameters of camera centers were estimated.

4. Building Detection

Many studies have been performed to detect buildings based on either single or multiple sensory data (Baltsavias *et al.*, 1995; Baillard *et al.*, 1998; Wang, 1998). From previous studies, it has been shown that detection methods using local neighborhood operations on image pixels have difficulties in choosing an optimal window size. Another approach is to use elevation contours. Liu and Ramirez (1997) used graph data structure to label the elevation tags of contours. Wu (1993) exploited graphs to extract vector contours from scanned maps.

In this study, graph structure is used to detect building regions because a contour-based method can provide building boundaries without gaps while the local filtering methods suffer from missing boundary pixels. Graph data structures representing the hierarchical inclusion relationships among adjacent contours are derived as follows. Firstly, closed contours are assigned to graph nodes. Secondly, the areas of closed contours are computed. Thirdly, two arbitrary contours are checked for an inclusion test. Fourthly, it is checked where the area and height conditions between two contours are reasonable. Fig. 2 illustrates an example of contours and a graph structure generated through the procedure. Finally, slopes among adjacent contours are computed at the graph edges and classified as either steep or non-steep. For more detail description, refer to Seo and Schenk (2003) and Seo (2003).

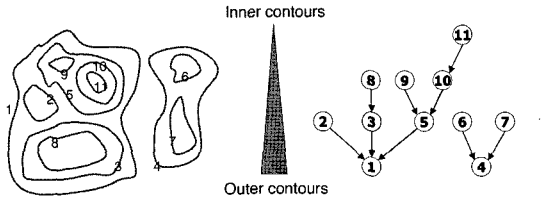

Fig. 2. A set of contours and its contour graph.

The proposed approach was tested with two lidar data sets. One has the point density of 0.0747 (points/m^2) and the other 1.0653 (points/m^2). The high density data is a subset of the lidar data described in Section 3. The low density data covers a residential area which contains low height buildings and the high density data a commercial area with a high story building and parking lots. Fig. 3 shows range images derived from the lidar data.

Contours were generated from the range images and classified according to slope values, whereby steep and non-steep contours were determined with the threshold value of 45 degrees. Among the classified contours, the contours whose slopes begin to be steeper than the specified threshold value are determined as detected building regions.

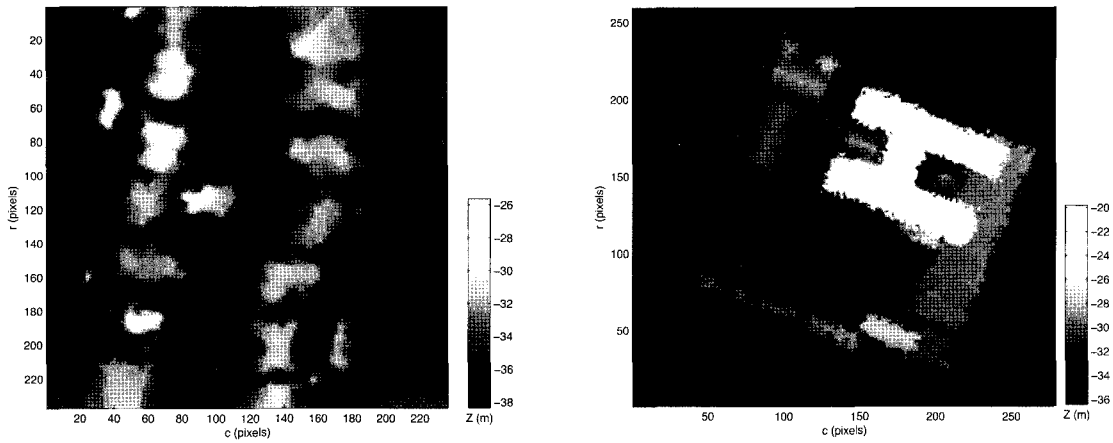

Fig. 3. Range images derived from lidar data. (a) shows a range image from low point density and (b) from high point density.

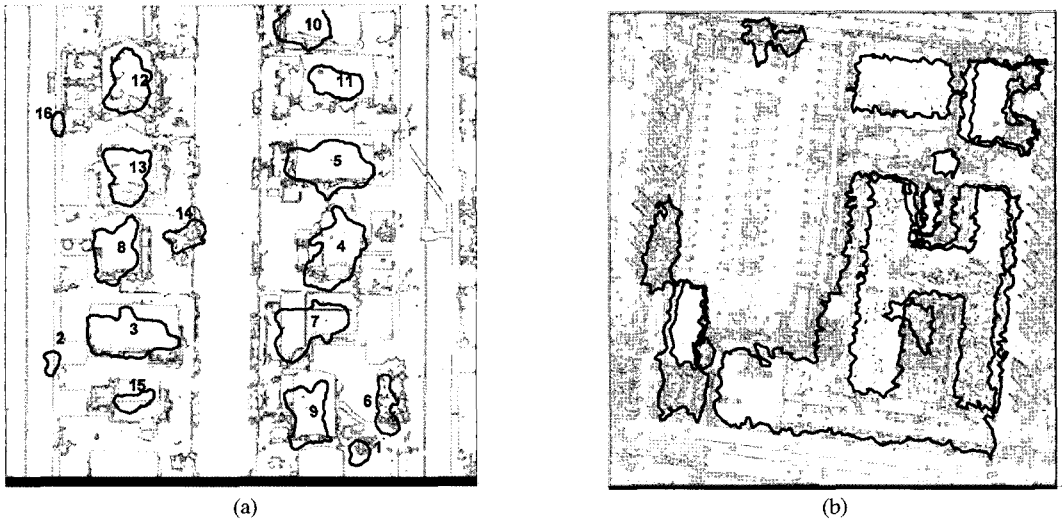

Fig. 4. Detected building regions by the contour-based approach.

Fig. 4 shows the contours detected as building areas back projected in exoskeleton images derived from the aerial images. As can be seen, building regions were detected successfully. One important advantage of this approach is that the elevation of external building boundaries can also be approximated, facilitating the subsequent building modeling process. The building regions can be pruned with comparison of the features in the aerial images. Visual inspection shows that in an automatic process the areas 4 and 5 can be accepted but the areas 6 and 14 should be discarded based on their neighboring straight line features.

5. Building Model Generation

Building modeling is one of the most important tasks for automating building reconstruction because of the complexity of building structures but the incompleteness of available features in sensory input data. Previous studies have shown that 3D surface

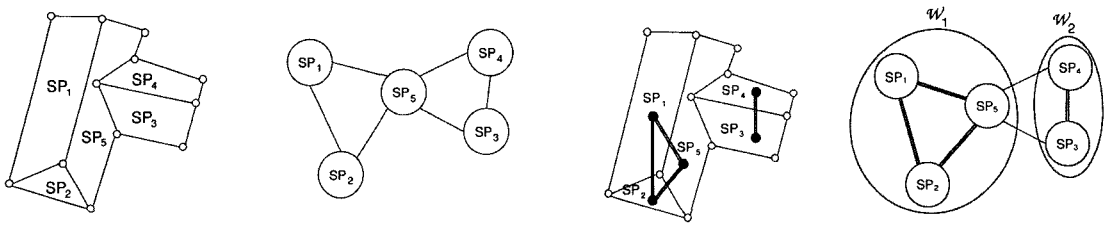

(a) (b)

Fig. 5. Surface patch adjacency graph. (a) Initial graph and (b) graph after building modeling.

patches are useful for modeling buildings because 3D surface patches can generate 3D lines and 3D corners by simply intersecting neighboring surface patches (Jaynes *et al.*, 1997; Ameri, 2000). Thus, in this study, the 3D surface patches from lidar are chosen as initial primitives for building model generation.

After segmenting lidar data into surface patches, adjacency relationships among the patches can be established. However, this study focuses on building modeling with segmented surfaces given. For details, refer to Brunn and Weidner (1998), Vosselman and Dijkman (2001), and Lee and Schenk (2001). Fig. 5-a shows an example of surface patch adjacencies represented in graph structure.

Here, to assemble planar surfaces into a complete building model, a wing model is proposed as an aggregation model. As compared with the corner model used by Fischer *et al.* (1998), whereby line features extracted from aerial images were aggregated around corners, the wing model proposed in this study assembles planar surface features around a wing. The wing model in this study is composed of two side surface patches whose azimuth angles are opposite and may have additional surfaces at the ends of the side patches, called end surface patches. The following describes the building modeling procedure based on the wing model.

1. Compute the degree of anti-symmetry among neighboring surface patches.
2. Start to generate wing models with a pair of surface patches with high anti-symmetric values.
3. Find ending surface patches of the initiated wing models in remaining surface patches.
4. Find junctions among the wing models and remaining surface patches.
5. Classify the type of wing models into gable, hip and junction.
6. Combining all wing models (Fig. 5-b).
7. Generate a complete building model by intersection the surface patches and the elevation contour found in the building detection process.

It should be noted, however, that up to Step 6, the shape of the building model is not delineated completely except the ridge lines at the intersections of patches. In order to delineate the eaves lines, an additional surface patch is required. The approach presented fulfills this requirement at Step 7 by adding a horizontal surface with the contour from building detection.

For experiments, building modeling was performed using the range image from the high density lidar data shown in Fig. 3-b. Here, the low density data shown in Fig. 3-a was not tested since it appears difficult to extract planar surface patches from the data. Fig. 6 shows the azimuth image of the high density data and surface patches obtained by visual observations. Parameters of the planar surface patches were estimated based on the LMedS (Least Median Square) method with a random sampling similar to the RANSAC (RANdom SAmple Consensus) method (Fischler and Bolles, 1981; Rousseeuw, 1984). For details, refer to Seo (2003).

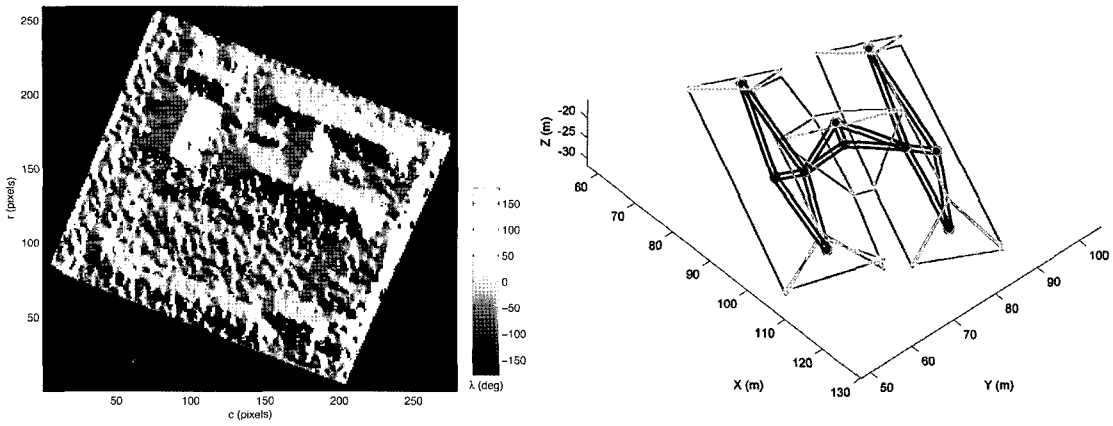

(a) (b)

Fig. 6. Planar surface patches. (a) shows an azimuth image derived from lidar data. (b) shows the surface patches extracted interactively (gray lines) and their adjacencies represented in graph data structure (black lines).

Fig. 8-a shows the surface derived from lidar data (upper left) and Fig. 8-b a building model generated by the above procedure.

6. Building Model Verification

In this study, in order to verify a building model, it is back projected into a pair of aerial images using their orientation parameters obtained from the co-registration process described in Section 3. After back projection, a building model is verified in terms of topology and geometry by comparing its entities with the features in aerial images. For checking the topology of the model, conditions about the connectivity and coplanarity of corners are added in equations, whereby each equation describes relationships among the coordinates of model entities and observed features. Geometric quality of a building model is evaluated based on the distance between the corners of a modeled building and those estimated by the model equations.

Fig. 7-a shows a building model back projected in the left side aerial image of test data. As can be seen,

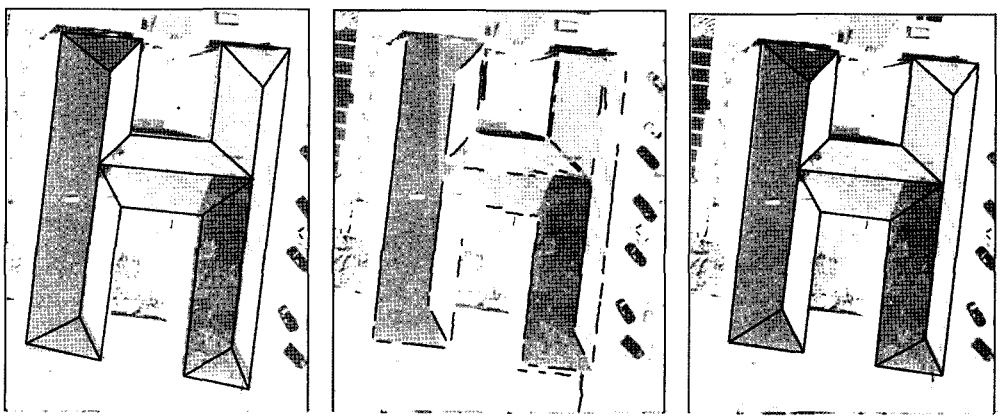

(a) (b) (c)

Fig. 7. Back-projection of a building model for verification. (a) shows a building model, (b) aerial image features extracted around the model, and (c) a building model verified and refined after the model verification process.

Table 2. Accuracy of the building corners from single and multi sensor data. Units are in centimeters.

Location	Lidar			Aerial Images			Lidar and Aerial Images		
	σ_X	σ_Y	σ_Z	σ_X	σ_Y	σ_Z	σ_X	σ_Y	σ_Z
Ridge Corners	11.64	6.40	2.10	19.97	18.47	48.18	21.99	12.71	4.85
Eaves Corners	153.42	148.17	100.00	13.30	15.38	39.48	24.62	22.71	14.52
All Corners	106.16	100.91	67.37	15.52	16.41	42.38	23.74	19.38	11.30
Radial Accuracy	161.22			48.02			32.66		

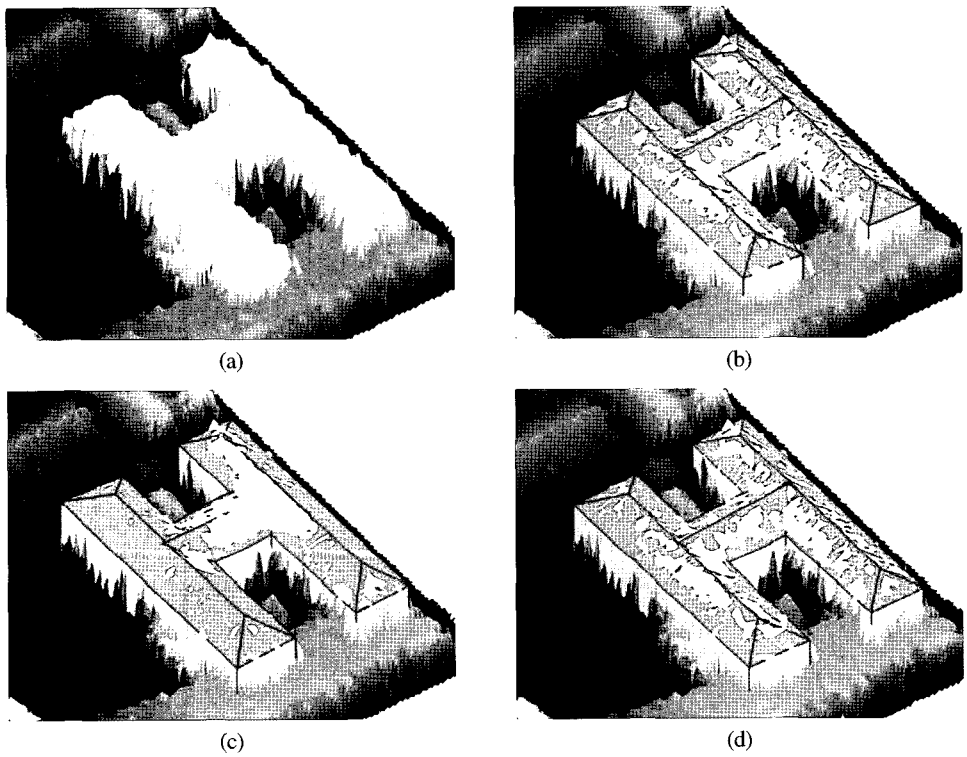

Fig. 8. Three-dimensional lidar surface and building models. (a) DSM from raw lidar data and comparison with building models (b) from lidar data only, (c) from aerial images only, and (d) from combination of lidar and aerial images. The DSM derived from raw lidar points is shown in gray scale whereby low areas are dark and high areas light. Building models are shown with two colors whereby roof surfaces are colored in dark gray and wall surfaces in light gray.

ridge lines of the building model correspond well to the building structure visible in the aerial image. However, some geometric discrepancies exist along the eaves lines. Table 2 summarizes the standard deviation at corner points of the building model. Here, it is notable that the standard deviations of the corners along eaves lines of the building model generated using lidar data are relatively large. This was caused by two factors: 1. Approximated elevation of eaves lines whose accuracy was considered as 1 meter because contours of 0.5 meter interval were used for detecting building regions. 2. Low number of points inside the ending surface patches. The back projected building model, however, makes a search space remarkably reduced to find its building features in aerial images.

In this study, in order to verify the model, straight lines are exploited. Fig. 7-b shows the straight lines from the edge detection and linking processes. Edge detection was performed using the Canny edge operator with sigma value 2.0 and filter size, 11 by 11. A binomial operator was used to speed up the process. After suppressing non-maxima edge pixels, the remaining pixels are linked into connected edges. During the edge linking process, straightness was considered at the junction of edges to extract long straight lines and lines shorter than a specified length were discarded. Then, straight line segments were extracted by iterative splitting and merging of the lines. As shown in Fig. 7-b, straight lines were detected well in the image. However, there are still many missing parts in building edges due to low contrast.

In this study, however, this problem is considerably resolved by integrating the edge entities of the building model from lidar data. Search regions are generated based on the back projected lines of the model. Here, buffers with 2m wide around the back projected model were generated and straight lines were collected inside the buffers.

Fig. 8-d shows a verified/refined building model. The refined model shows the geometric closeness to the raw surface and similar to the model generated by lidar data only. Detail examination, however reveals that there are geometric differences between the two models, in particular, along the external boundary of the model (Table 2). In order to compare the quality of building modeling using single and multiple sensors, a building model was extracted manually using only aerial images (Fig. 8-c). Then, qualities of the building models were compared based on the corners.

Table 2 summarizes their accuracies by the average standard deviations of corner locations, whereby the 18 corners of the model were classified into 6 ridge and 12 eaves corners. The ridge corners are located along ridge lines and their locations were determined by intersecting three surface patches. The eaves corners are located along eaves lines and their locations were computed by intersecting two roof surface patches and the plane of the building boundary contour. As can be seen, the geometric quality of the building model from aerial images is lower in the vertical direction as compared with the model from lidar data only. From the experiments, the fusion-based method presented is shown to deliver more accurate building models than methods based on single sensor data.

7. Concluding Remarks

In this paper, a fusion-based building extraction method was presented using aerial images and lidar data. Regarding building detection, the analysis of contour graph was shown as an efficient method to detect building regions. In building modeling, the result proves that building structures can be established well by using the anti-symmetric property of roof surface patches. In building model verification, the building model generated from lidar was verified based on the features from aerial images. Also, the model generated could provide correspondence between left and right images directly without matching process, which saved the time for finding corresponding features between images.

Furthermore, the model resolved the problems of missing features in aerial images such as crease edges due to low contrast by providing topological relationships among the corners and edges, which definitely benefited the extraction of a generic type of building models. In addition, given the model, the features in aerial images were shown useful to

validate the model in terms of topology and geometry and to improve the localization quality of the model.

References

Abidi, M. A. and R. C. Gonzalez, 1992. *Data Fusion in Robotics and Machine Intelligence*, Academic Press, San Diego, 546 p.

Ameri, B., 2000. *Automatic Recognition and 3D Reconstruction of Buildings Through Computer Vision and Digital Photogrammetry*, Ph.D. Dissertation, University of Stuttgart, Stuttgart, Germany, 110 p.

Baltsavias, E. P., S. O. Mason, and D. Stallmann, 1995. Use of DTMs/DSMs and orthoimages to support building extraction, *Automatic Extraction of Man-Made Objects from Aerial and Space Images* (A. Grun, O. Kubler, and P. Agouris, editors), Birkaeuser, Basel, pp.199-210.

Baillard, C., O. Dissard, O. Jamet, and H. Maitre, 1998. Extraction and textural characterization of above-ground areas from aerial stereo pairs: a quality assessment, *ISPRS Journal of Photogrammetry and Remote Sensing*, 53(2): 130-141.

Brunn, A. and U. Weidner, 1998. Hierarchical Bayesian nets for building extraction using dense digital surface models, *ISPRS Journal of Photogrammetry and Remote Sensing*, 53(5): 296-307.

Csatho, B., W. Krabill, Lucas, J., and T. Schenk, 1998. A multisensor data set of an urban and coastal scene, *International Archives of Photogrammetry and Remote Sensing*, 32(Part 3/2): 26-31.

Csatho, B., T. Schenk, D.-C. Lee, and S. Filin, 1999. Inclusion of multispectral data into object recognition, *International Archives of Photogrammetry and Remote Sensing*, 32(Part 7-4-3 W6): 53-61.

Brenner, C. and N. Haala, 1998. Fast production of virtual reality city models, *IAPRS Commission IV Symposium on GIS*, Stuttgart, Germany, pp. 77-84.

Brunn, A., E. Gulch, F. Lang, and W. Foestner, 1998. A hybrid concept for 3D building acquisition, *ISPRS Journal of Photogrammetry and Remote Sensing*, 53(2): 119-129.

Fischer, A., T. H. Kolbe, Lang F., A. B. Cremers, W. Foestner, L. Plumer, and V. Steinhage, 1998. Extracting buildings from aerial images using hierarchical aggregation in 2D and 3D, *Computer Vision and Image Understanding*, 72(2): 185-203.

Fischler, M. A. and R. C. Bolles, 1981. Random sample consensus: A paradigm for model fitting with application to image analysis and automated cartography, *Communications of the ACM*, 24(6): 381-395.

Haala, N. and C. Brenner, 1999. Extraction of buildings and trees in urban environments, *ISPRS Journal of Photogrammetry and Remote Sensing*, 54: 130-137.

Jaynes, C., E. Riseman, and A. Hanson, 1997. Building reconstruction from optical and range images, *Computer Vision and Pattern Recognition*, San Juan, Puerto Rico, pp. 374-379.

Lee, I. and T. Schenk, 2001. 3D perceptual organization of laser altimetry data, *International Archives of Photogrammetry and Remote Sensing*, 34(Part 3/ W4): 57-65.

Liu, X. and J. Ramirez, 1997. Automated vectorization and labeling of very large hypsographic map images using a contour graph, *Surveying and Land Information*

Systems, 57(1): 5-10.

Mckeown, D. M., S. D. Cochran, S. J. Ford, J. C. McGlone, J. A. Shufelt, and D. A. Yocum, 1999. Fusion of HYDICE hyperspectral data with panchromatic imagery for cartographic feature extraction, *IEEE Trans. on Geoscience and Remote Sensing*, 37(3): 1261-1271.

Rousseeuw, P. J., 1984. Least median of squares regression, *Journal of the American Statistical Association*, 79(388): 871-880.

Schenk, T. and B. Csatho, 2002. Fusion of LIDAR data and aerial imagery for a more complete surface description, *International Archives of Photogrammetry and Remote Sensing*, 34(Part 3A): 310-317.

Seo, S., 2003. *Model-Based Building Extraction from LIDAR and Aerial Imagery*, Ph.D. Dissertation, The Ohio State University, Columbus, Ohio, 138 p.

Seo. S. and T. Schenk, 2003. A study of integration methods of aerial imagery and LIDAR data for a high level of automation in 3D building reconstruction, *Proceedings of the SPIE*, 5099: 65-76.

Tao, G. and Y. Yasuoka, 2002. Combining high resolution satellite imagery and airborne laser scanning data for generating bareland DEM in urban areas, *International Archives of Photogrammetry and Remote Sensing*, 34(Part 5/W3), unpaginated CD-ROM.

Vosselmann, G. and S. Dijkman, 2001. 3D building model reconstruction from point clouds and ground plans, *International Archives of Photogrammetry and Remote Sensing*, 34(Part 3/W4): 37-43.

Wang, Z., 1998. Extracting building information from LIDAR data, *International Archives of Photogrammetry and Remote Sensing*, 32(3/1): 279-284.

Wu, C.-H., 1993. *Automated Identification of Scanned Contour Information for Digital Elevation Models*, Ph.D. Dissertation, University of Maine, Orono, Maine, 120 p.